Transactions, **SMiRT-26**
Berlin/Potsdam, Germany, July 10-15, 2022
Division V

LOCAL FAILURE ANALYSES OF 1/4 SCALED PCCV UNDER A TYPICAL SEVERE ACCIDENT CONDITION

Woo-Min Cho[1], Yoon-Suk Chang[1, †]

[1] Department of Nuclear Engineering, Kyung Hee University, 1732 Deogyeong-daero, Giheung-gu, Yongin-si, Gyeonggi-do 17104, Republic of Korea (dnals0509@khu.ac.kr; yschang@khu.ac.kr)

ABSTRACT

Containment building is a final shielding structure for nuclear power plant in the event of severe accidents. Extensive researches have been conducted on the overall behaviour of the structure subjected to the internal pressure. In this paper, local failure of a 1/4 scaled Prestressed Concrete Containment Vessel (PCCV) was assessed based on previous test data. Despite numerous studies were conducted on the same containment model, the local regions such as Equipment Hatch (EH) and Airlock (AL) were barely spotlighted as the complex geometries created difficulties in evaluation. For more efficient and accurate analyses, local model based on the results of global model was implemented using sub-modeling technique. Two Finite Element (FE) models like Total-Coarse (T-C) model and Liner-Fine (L-F) model were developed, and utilized to evaluate the strains of liner. Also, effects of liner degradation have been investigated. Thickness reduction of liner was considered to where tears occurred, which were resulted in the significant amount of strain elevation.

INTRODUCTION

Since the containment building is a final barrier to withstand all the static load exceeding design bases in the event of severe accidents, accurate analysis of the failure behaviour of the containment building is necessary. Thus, numbers of experimental and numerical studies on various scaled containments have been performed to properly cope with the unlikely event of a severe accident. Among them, the 1/4 scaled Prestressed Concrete Containment Vessel (PCCV) test by Sandia National Laboratories (SNL) analysed the failure modes and mechanical behaviour of containment structures subjected to increasing internal pressure (Hessheimer, M. F. et al., 2003). As the test progressed, the functional failure occurred due to cracks in concrete and tears of the liner attached to the inner surface of containment building for its leak-tightness. The test was ended when the structural failure occurred by the rupture of the tendon. Strain-based failure criteria obtained from a global displacement measured at each failure mode was suggested but is not suitable for evaluating the failure in the vicinity of discontinuities where local stress and strain concentration occurs (NRC, 2010). Meanwhile, the reduction of liner thickness due to grinding and welding has been found to be significant for the leak tightness capacity (Spencer, B. W. et al., 2006). Also, in Korea, a few nuclear power plants have been reported for the degradation of the liner (Paek, Y. L. et al., 2018).

This study aims to evaluate the liner failure of tears near discontinuities where stress and strain concentration occurs and the effects of thickness reduction of liner, using Total-Coarse (T-C) model with discontinuities such as Equipment Hatch (EH) and Liner-Fine (L-F) model. A nonlinear finite element analysis using commercial software ABAQUS was performed to figure out the failure behaviour of containment building and analysis results were compared with the test (ABAQUS-6.12., 2018). The displacement-pressure histories obtained from a T-C model were used for the boundary conditions of L-F model. The numerical result of the liner strain was compared with the test results. Moreover, the influence of the liner degradation by degrees of thickness on the strain elevation was evaluated.

Test program

The 1/4 scaled PCCV is depicted in Fig. 1 (Hessheimer, M. F. et al., 2003). The model was 16.4 m high, had a 1.075 m inner diameter and the concrete wall was a 0.325 m thick. On the inside surface of the concrete wall, a 1.6 mm steel liner was attached, acting as a leak-tightness membrane. The rebar and tendon were embedded in the concrete wall. Including two buttresses, the structure had two major penetrations (EH and Airlock; AL), along with minors (Main Steam; MS and Feed Water; FW).

In the overpressurization test, the internal pressure was loaded up to 3.3 times the design pressure (P_d = 0.39 MPa). At 3.3 P_d, numbers of liner tears occurred and the test was terminated as the leak rate exceeded the pressurization capacity of the system. Figure 2 shows the liner tear locations seen from the inside of the model at 3.3 P_d. The major region where failure occurred was near the discontinuities. There were various factors causing failure and for tears #7 and #15, the thickness reduction due to the grinding and welding was reported as the main reason for failure.

Finite element modeling of the 1/4 scaled PCCV

Two Finite Element (FE) models were developed and analysed. T-C model was developed to figure out the overall structure behaviour at the free field and near discontinuities. The FE model generation followed the guideline for determining the internal pressure capacity using an analytical technique (Hessheimer, M. F. and Dameron, R. A., 2006). All components including concrete wall, liner, rebar and tendon were considered. Then, the L-F model where only liner was considered was generated based on the results of the T-C model, especially displacement which was interpolated onto the boundary of the L-F model. The liner strain was compared with the test so that the necessity and accuracy of L-F model was proven. With the finest mesh, the effects of liner degradation which was reported after the test were investigated.

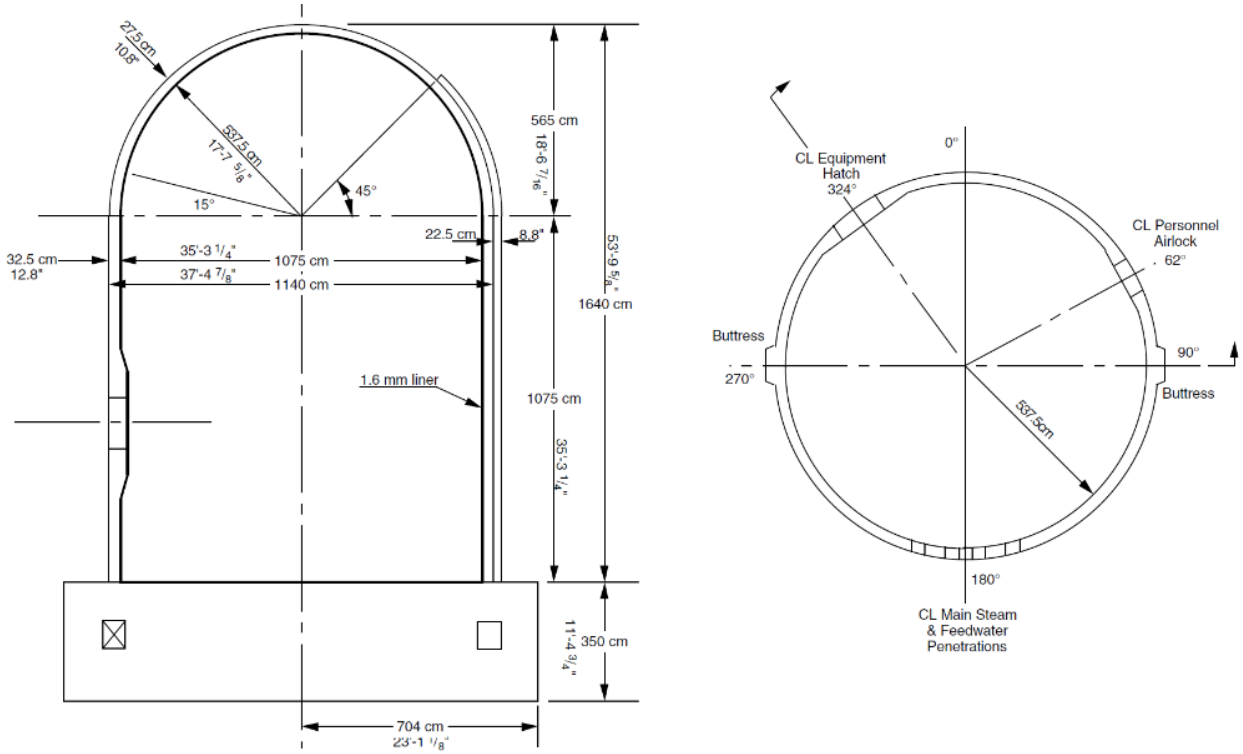

Figure 1. Geometry of the 1/4 scaled PCCV model (Hessheimer, M. F. et al., 2003).

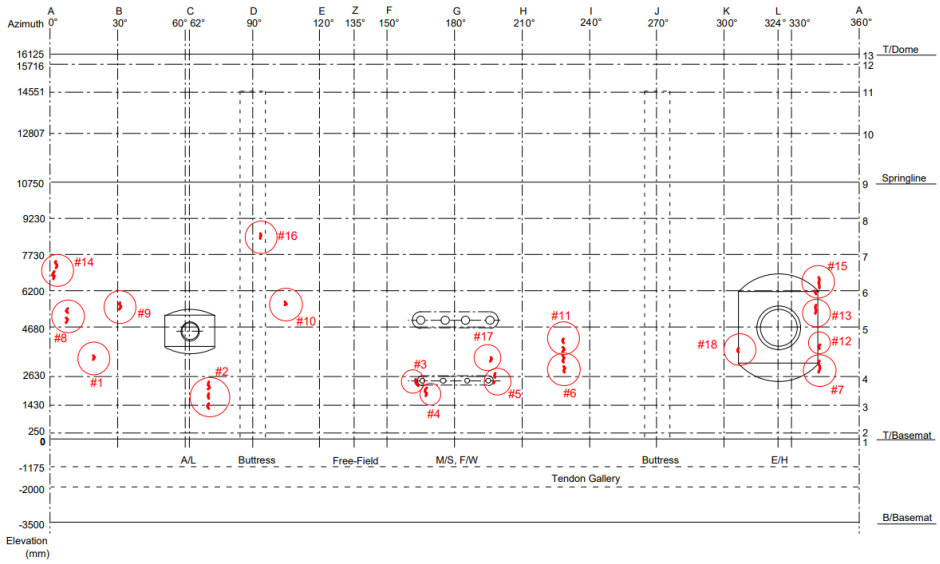

Figure 2. Stretched-out liner tear locations of the 1/4 scaled PCCV (Hessheimer, M. F. et al., 2003).

Three loads were considered in this study. The bodyweight was applied for each component. Then, the tendon prestressing values of 897.52 MPa and 1,250.50 MPa, considering the losses from creep and relaxation, were assigned to the horizontal and vertical directions which ensure the structure to resist tensile stress. Finally, the internal pressure up to 3.3 P_d was loaded perpendicular to the inner surface of the liner. The degrees of freedom of whole elements and nodes at the bottom surface were constrained. The rebars and tendons were constrained in the concrete using the embedded element option. The concrete was designated as 8 nodes three-dimensional stress elements (C3D8), 4 nodes three-dimensional (M3D4) elements type was used for the liner, and rebar was meshed with 2 nodes three-dimensional truss elements (T3D2) along horizontal and vertical directions. There were total 165,117 elements and 170,940 nodes in the present T-C model. The comprehensive FE model of 1/4 scaled PCCV is shown in Fig. 3.

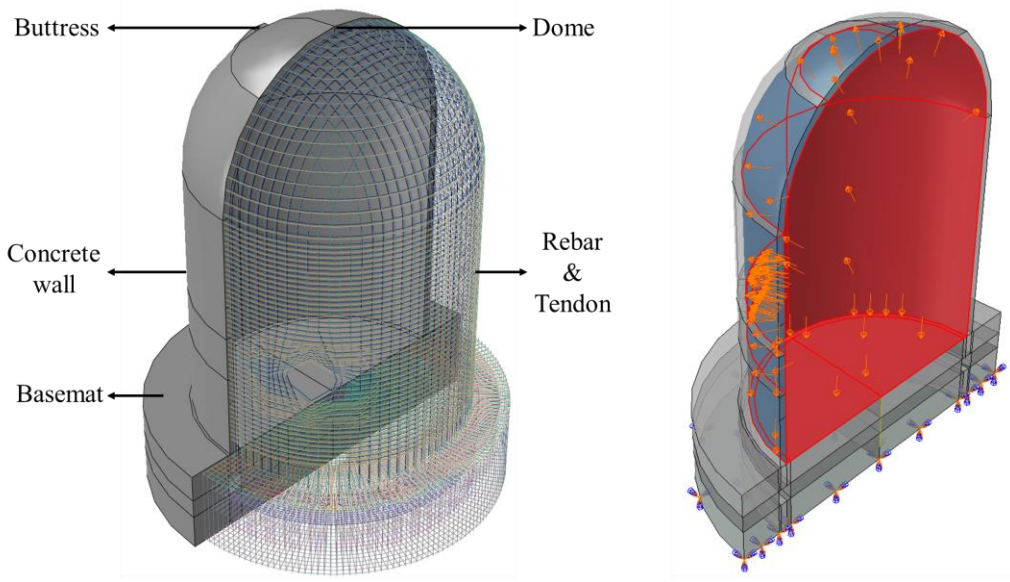

(a) Total-Coarse (T-C) model (b) Loading and boundary conditions

Figure 3. The comprehensive FE models of 1/4 scaled PCCV.

Constitutive material models

Concrete

The constitutive concrete material model developed by Hognestad was adopted for compression in this numerical study (Hognestad, E., 1951). This constitutive model simulates the behaviour of confined concrete after yielding. The following Hognestad equations are the parabola less than the strain at the ultimate strength (ε_0) and a straight line up to the ultimate compressive strain (ε_{cu}), which is typically taken as 0.0038. The ultimate compressive strength of concrete is expressed as f_c.

$$\sigma_c = \begin{cases} f_c\left[2\left(\frac{\varepsilon}{\varepsilon_0}\right) - \left(\frac{\varepsilon}{\varepsilon_0}\right)^2\right] for\ \varepsilon \le \varepsilon_0 \\ f_c\left(1 - 0.15\frac{\varepsilon - \varepsilon_0}{\varepsilon_{cu} - \varepsilon_0}\right) for\ \varepsilon_0 < \varepsilon < \varepsilon_{cu} \end{cases} \quad (1)$$

Here, the yield point of $0.4 \times f_c$ was assumed due to nearly the straight line at initial loading phase, which has been implemented by other researches (Alhanaee, S. et al., 2018).

Tensile behaviour of concrete was simulated by implementing the Izumo model to formulate the nonlinear response, which accounts for the tension stiffening (Izumo, J. et al., 1989). The equations are the constant from the cracking strain (ε_{cr}) to the double of it and exponential function up to the ultimate tensile strain as defined by the following equations.

$$\sigma_t = \begin{cases} f_t & for\ \varepsilon_{cr} < \varepsilon \le 2\varepsilon_{cr} \\ \left(\frac{2\varepsilon_{cr}}{\varepsilon}\right)^c \times f_t & for\ 2\varepsilon_{cr} < \varepsilon \end{cases} \quad (2)$$

where f_t is the ultimate tensile strength of concrete and the constant c was 0.4 as implemented by previous researches (Matsubayashi, M. et al., 2020).

In this study, Concrete Damaged Plasticity (CDP) model, which provides the general capability for concrete and can be used in conjunction with rebar, was adopted to appropriately simulates the behaviour of concrete structure (ABAQUS-6.12., 2018). Parameters of the density, Young's modulus, Poisson's ratio, ultimate compressive strength, and plasticity used for the CDP model are listed in Table 1.

Table 1. Material properties of concrete (Spencer, B. W. et al., 2006).

Density	Young's modulus	Poisson's ratio	Ultimate compressive strength
2.176×10^{-9} ton/mm^3	27,200 MPa	0.21	48.85 MPa
Dilatation angle	Eccentricity	Ratio of biaxial to uniaxial compressive strength	Invariant ratio
34	0.1	1.16	0.667

Steels

A plasticity model independent of strain rate with isotropic hardening based on the von-Mises yield surface was considered for nonlinear behaviours of rebar, liner and tendon of 1/4 scaled PCCV model (ABAQUS Inc, 2018). The characteristic of isotropic hardening discusses the uniform distribution of the yield stress in all directions when the plastic strain occurs. Their densities, Young's moduli, Poisson's ratios, and yield strengths are listed in Table 2.

Table 2. Material properties of steels (Hessheimer, M. F. et al., 2003; Spencer, B. W. et al., 2006).

Component	Density	Young's modulus	Poisson's ratio	Yield strength
Rebar	7.85×10^{-9} ton/mm^3	200,000 MPa	0.3	460.0 MPa
Liner	7.81×10^{-9} ton/mm^3	220,000 MPa	0.3	376.2 MPa
Tendon	7.41×10^{-9} ton/mm^3	195,200 MPa	0.3	1,592.7 MPa

Analysis results of T-C model

The T-C model was developed to evaluate the overall behaviour of the structure and to derive results for submodels. Figure 4(a) shows the free field radial displacement contour of liner calculated from the T-C model analysis and Fig. 4(b) shows the radial displacement contour of concrete near EH (right) at an internal pressure of 3.3 P_d (1.29 MPa). To confirm that the T-C model was reliable, test data was compared with the FE results. The free field region at the elevation of 6,200 mm and an azimuth of 135 degrees where is far away from discontinuities including the EH and AL was chosen for comparison. As a result, the T-C model was compatible with the test data as the maximum radial displacement resulted from FEA was 23.669 mm and the test result was 23.402 mm which differed by 1.14%.

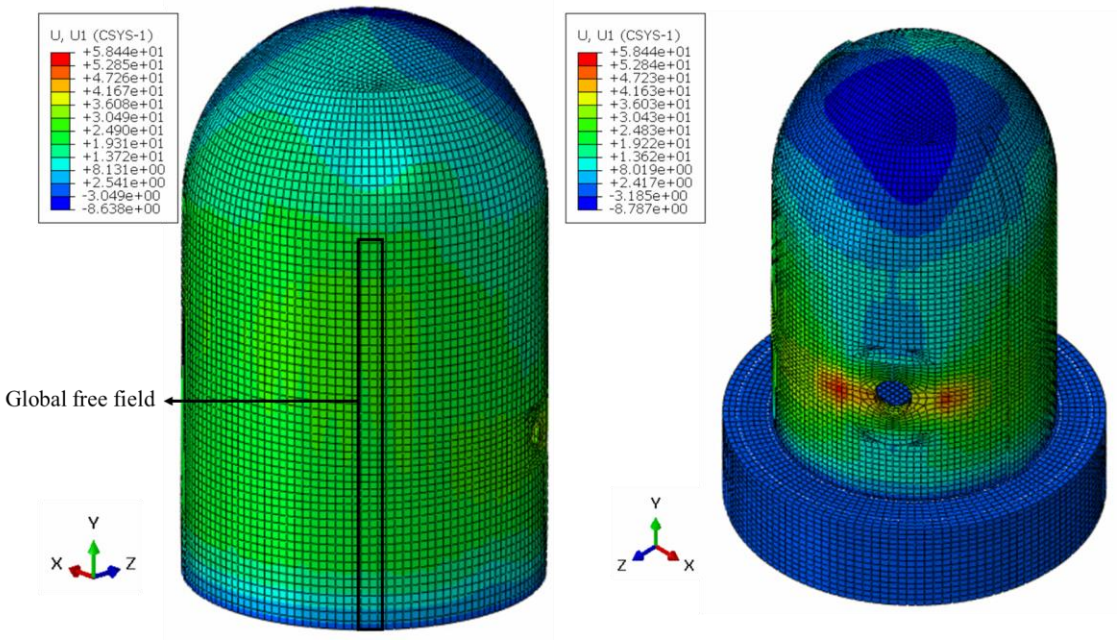

(a) Free field region (liner) (b) EH region (concrete)

Figure 4. Radial displacement contours of Total-Coarse (T-C) model (unit: mm).

Analysis results of L-F model

Sub-modeling technique that ABAQUS provides has been applied for the L-F model. This technique uses results of the T-C model as a displacement load for the L-F model. The driven region of boundary condition was from all overlapping area with the T-C model. Only liner for EH was modelled for the most accurate and conservative results. FE models with four mesh sizes (2.5 mm, 5 mm, 10 mm and 75 mm) were generated and the convergence of solution was investigated. Figure 5 shows liner strain contours where peak values occurred according to different FE models. The liner strain for 2.5 mm mesh size increased 0.001% compared with the 5.0 mm mesh size and was considered as converged. The L-F model with 2.5 mm mesh size resulted in 3.77% of maximum hoop strain and agreed with the test results which indicated that the maximum liner strain at the EH was 3.88%. For the degradation analysis, the right-half of EH was modelled and there were 751,120 elements and 753,134 nodes in the L-F model.

Aiming at the most accurate numerical analysis with developed L-F model, the finest mesh size was chosen for the study of liner degradation effects. Liner tears of #7 and # 15 which are shown in Fig. 2 were investigated. In these regions, complex stresses and strain concentrations occurred and liner thinning from grinding, repair welding was also expected. The post inspection of the overpressurization test indicated that several degradations were observed near the lower (#7) and upper (#15) corners of the EH transition joint. Liner degradations in thickness reduction of 30% at tear #7 and 50% at tear #15 were discovered out.

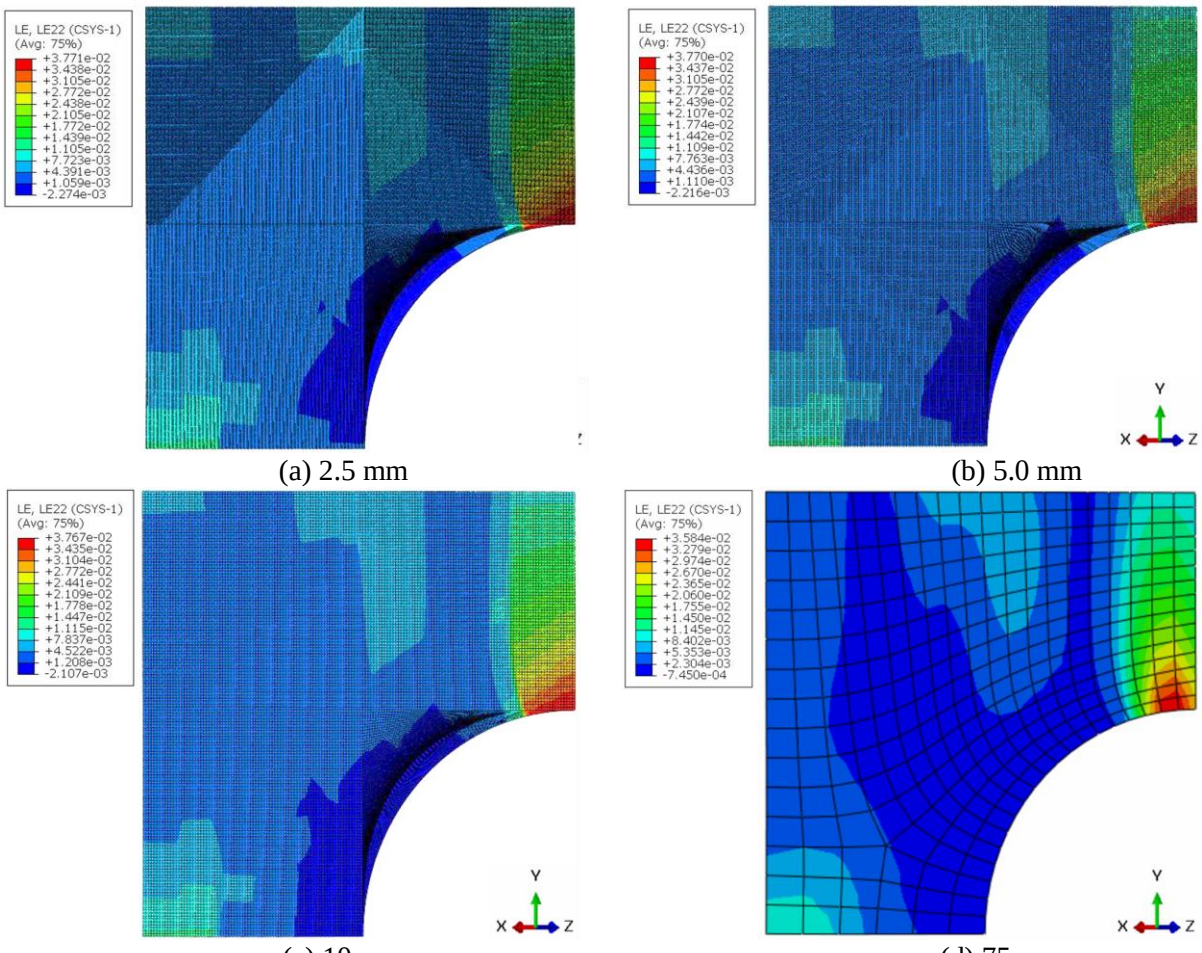

(a) 2.5 mm (b) 5.0 mm

(c) 10 mm (d) 75 mm

Figure 5. Liner hoop strain distributions of Liner-Fine (L-F) model according to mesh sizes.

To evaluate the influence of liner degradation, thickness reductions of the same degrees were applied to corresponding regions and analysed. In Fig. 6, The strains in the hoop direction of liner derived from the T-C model and L-F model for tears #7 and #15 are plotted. The liner strains increased as the model became sophisticated for both tears #7 and #15, and there were significant strain elevations when degradations were applied. For tear #7, the liner hoop strain increased from 0.00692 (T-C model) and 0.00903 (L-F model, no degradation) to 0.02571 (L-F model, 30% thickness reduction). For tear #15, the liner strain increased from 0.00304 (T-C model) and 0.00473 (L-F model, no degradation) to 0.02016 (L-F model, 50% thickness reduction). Using L-F model, the hoop strain of tears #7 and #15 was elevated by 30.4% and 55.5%, compared with the results of T-C model. Also, 30% and 50% liner thickness reductions increased the strains of liner by 2.84 and 4.26 times.

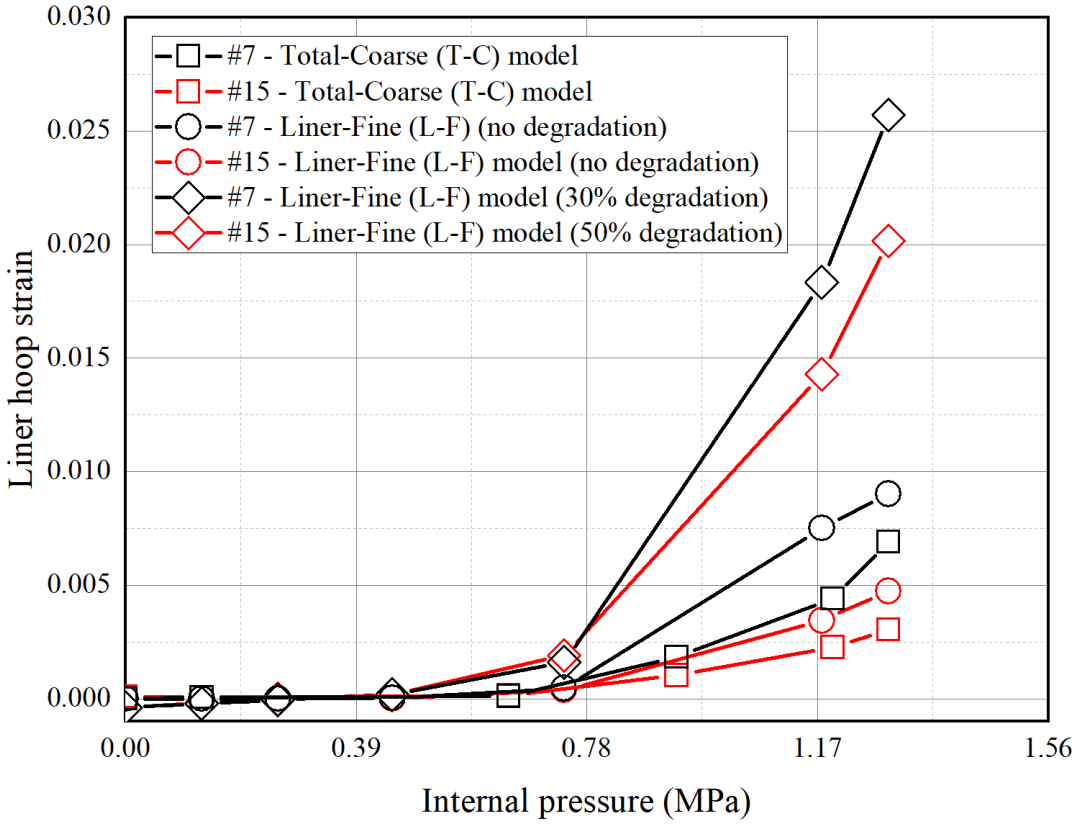

Figure 6. Liner hoop strains for tears #7 and #15 evaluated by different FE models.

CONCLUSION

The following FE models were developed and analysed in this study.

- Total-Coarse (T-C) model
- Liner-Fine (L-F) model

The T-C model was developed, for which all components including concrete, liner, rebar and tendon was included in the model. Also, the discontinuities such as EH, AL and buttresses were considered so that the result of T-C model can be utilized for the L-F model. With regard to this model, it was verified that the numerical simulation is enough to describe the overall behaviour of containment building by comparing the radial displacement at the elevation of 6,200 mm and an azimuth of 135 degrees.

The L-F model was developed for the accurate evaluation of liner strains and the effects of degradation in thickness which cannot be precisely evaluated with the T-C model. Tears #7 and #15 were investigated in which 30% and 50% of thickness reduction was observed, respectively. For this, L-F model with the mesh size of 2.5 mm, which is the 1/100 of the T-C model mesh size of 250 mm, was utilized. The L-F model concluded in the elevations of hoop strains by 30.4% and 55.5% for tears #7 and #15, compared with the results of T-C model. The degradations of 30% and 50% of thickness reduction increased the strains by 2.84 and 4.26 times larger than those in which no degradation was applied. Thus, it was considered that the L-F model should be used for precise evaluation and there could be a significant amount of liner strain increase by the degradation of liner thickness reduction due to various reasons such as grinding and welding.

Acknowledgements

This work was supported by the Nuclear Safety Research Program through the Korea Foundation Of Nuclear Safety (KoFONS) using the financial resource granted by the Nuclear Safety and Security Commission (NSSC) of the Republic of Korea (No. 2106034).

REFERENCES

ABAQUS-6.12. (2018). ABAQUS Analysis User's Manual. ABAQUS 6.12, Dassault Systèmes Simulia Corp., Providence, RI, USA.

Alhanaee, S., Yi, Y. and Schiffer, A. (2018). "Ultimate Pressure Capacity of Nuclear Reactor Containment Building under Unaged and Aged Conditions," *Nuclear Engineering and Design*, 335: 128-139.

Hessheimer, M. F. and Dameron, R. A. (2006). "Containment Integrity Research at Sandia National Laboratories - An Overview," Technical Report No. NUREG/CR-6906, SAND2006-2274P. U.S. Nuclear Regulatory Commission, Washington, DC, USA.

Hessheimer, M. F., Klamerus, E. W., Lambert, L. D. and Rightley, G. S. (2003). "Overpressurization Test of A 1:4-Scale Prestressed Concrete Containment Vessel Model," NUREG/CR-6810, SAND2003-0840P.

Hognestad, E. (1951). "A Study on Combined Bending and Axial Load in Reinforced Concrete Members," University of Illinois at Urbana-Champaign, IL, 43–46. Bulletin.

Izumo, J., Shima, H. and Okamura, H. (1989). "Analytical Model for RC Panel Elements subjected to In-plane Forces," *Concrete Library Japan Society of Civil Engineers*, 12: 155–181.

Matsubayashi, M., Takase, Y. and Mizoguchi, M. (2020). "Shear Strength and Cracking Behaviour of Reinforced Concrete Non-structural Walls," *Journal of Asian Architecture and Building Engineering*, doi: 10.1080/13467581.2020.1838290.

NRC. (2010). Regulatory Guide 1.216. "Containment Structural Integrity Evaluation for Internal Pressure Loading above Design-Basis Pressure," U.S. Nuclear Regulatory Commission.

Paek, Y. L., Kim, S. Y., Yoon, E. S. and Cha. H. (2018). "Introduction of Containment Liner Plate (CLP) Corrosion," *Transactions of the Korean Nuclear Society Spring Meeting*, Jeju, Korea, May 17-18.

Spencer, B. W., Petti, J. P. and Kunsman, D. M. (2006). "Risk-Informed Assessment of Degraded Containment Vessels," NUREG/CR-6920, SAND2006-3772P.